Published version available at: https://doi.org/10.1016/j.combustflame.2021.111643

Flame initiation near a cold isothermal wall: ignition by an instantaneous thermal dipole

Vadim N. Kurdyumov [1a], Carmen Jiménez [a], Mario Sánchez-Sanz [b]

[a]*Department of Energy, CIEMAT, Avda. Complutense 40, 28040 Madrid, Spain*

[b]*Fluid Mechanics Group, Universidad Carlos III de Madrid, Avda. de la Universidad 30, Leganés, Spain*

Abstract

The ignition process produced by the instantaneous application of a linear local heat source near a cold wall is studied using irreversible Arrhenius kinetics. Special attention is devoted here to investigate the limiting case when the source is located at a distance from the wall small in comparison with the thermal width of the flame. The ignition problem in this case is reduced to the study of flame initiation by means of a thermal dipole. Changes in the critical values of the dipole intensity for successful ignition are presented as a function of the Lewis number. The results are compared with the configuration in which the distance between the source and the cold wall is finite. This study is also relevant for safety issues in the sense of preventing accidental ignition of combustible mixtures.

1 Introduction

Igniting a combustible mixture is a fundamental step in many technological processes. This can be done in a variety of ways, and one of the most common is through the application of a localized source of thermal energy.

Although research on the ignition of mixtures can be traced back to more than seventy years ago [1–3], only when numerical methods of analysis were applied to this problem it became possible to clarify many details of this process [4–8]. The development of asymptotic methods has also made a great contribution to the understanding of ignition processes [9, 10], as well as the application of analytical methods to simplified models [11]. Considerable attention was paid to ignition processes using concentrated and local heat sources, as well as to the determination of the minimum energy required for a successful ignition [6–8, 12–16]. In a recent work [17],

[1]Corresponding author

the application of a localized heat source to initiate the combustion process in a boundary layer was studied with application to micro-combustion devices.

In ignition research, the location for the heat source is usually selected away from possible heat sinks. In cases where the source must be located near a body, for example a wall, most models assume that it is adiabatic. Obviously, all this is done to increase the efficiency of the heat source for ignition. However, these theoretical configurations often turn out to be poorly consistent with the real conditions appearing in experiments or in technological processes.

In the present study, the ignition of a combustible mixture is investigated under conditions in which an instantaneously concentrated linear heat source is placed near a cold wall. The thermal conductivity of the wall is considered high enough to ensure its constant (cold) temperature. If the heat source is located at a small distance from the wall, in comparison with the thermal width of the flame, to be defined in the following section, then the effect of this source is equivalent to the action of a thermal dipole located on the wall. According to the authors' knowledge, this kind of ignition configuration has not yet been investigated in the literature, despite the many studies conducted on the ignition phenomenon.

The article is structured as follows. The next section presents the mathematical formulation of the problem. Section 3 presents transformations of independent variables used in the numerical analysis along with numerical modeling details. The results of the numerical analysis are presented in Section 4. The last Section provides conclusions and considers possible options for further research. The Appendix presents the results of simulating ignition using an isolated line source.

2 Formulation

Consider a quiescent gaseous reacting mixture near a cold isothermal wall. The wall is kept at the temperature T_0 which remains the same all the time. This can be done, for example, by means of a highly conductive wall material. The mixture has an initial temperature equal to the wall temperature and an initial fuel mass fraction Y_0. The initial state of the mixture is disturbed by the local instantaneous application of thermal energy in the form of a line situated parallel to the wall at distance H. Thus the energy source is parallel to the $\tilde{z}$ direction and all spatial distributions of the dependent variables are assumed to be two-dimensional, $f = f(\tilde{x}, \tilde{y}, \tilde{t})$, where $\tilde{x}$ and $\tilde{y}$ denote the spatial coordinates along and perpendicular to the wall, respectively, and $\tilde{t}$ is the time. Here and below "$\sim$" is used to denote dimensional variables if the same notations are used for dimensional and dimensionless variables.

Assuming that the mixture is lean in fuel, the oxidizer mass fraction remains nearly constant in the following. The amount of fuel consumed per unit volume and per unit time is given by $\Omega = \mathcal{B}\rho^2 Y \exp(-\mathcal{E}/\mathcal{R}T)$, where $\mathcal{B}$ is a pre-exponential factor, ρ is the density of the mixture, $\mathcal{E}$ is the overall activation energy and $\mathcal{R}$ is the universal gas constant. This work deals with a diffusive-thermal or "constant-density" model, according to which the density of the mixture ρ, the heat capacity c_p, the fuel thermal diffusivity $\mathcal{D}_T$, and the molecular diffusivity $\mathcal{D}$ are all assumed constant.

To describe the ignition process in a dimensionless form, the burning velocity of the planar flame, S_L, and the thermal flame thickness defined as $\delta_T = \mathcal{D}_T/S_L$ are used below to specify the non-dimensional parameters. The nondimensional temperature is defined as $\theta = (T - T_0)/(T_a - T_0)$, where $T_a = T_0 + QY_0/c_p$ is the adiabatic temperature of the planar flame. Choosing δ_T and $\delta_T^2/\mathcal{D}_T$ as the reference length and time scales, $(x, y) = (\tilde{x}/\delta_T, \tilde{y}/\delta_T)$, $t = \tilde{t}\,\mathcal{D}_T/\delta_T^2$, and Y_0 to normalize the fuel mass fraction, the dimensionless equations become

$$\frac{\partial \theta}{\partial t} = \Delta\theta + \omega, \tag{1}$$

$$\frac{\partial Y}{\partial t} = Le^{-1}\Delta Y - \omega, \tag{2}$$

where $\Delta = \partial^2/\partial x^2 + \partial^2/\partial y^2$ and

$$\omega = \frac{\beta^2}{2Le u_p^2} Y \exp\left\{\frac{\beta(\theta - 1)}{1 + \gamma(\theta - 1)}\right\} \tag{3}$$

is the dimensionless reaction rate.

The boundary conditions on the wall and in the distance are

$$y = 0: \quad \theta = \partial Y/\partial y = 0; \quad \sqrt{x^2 + y^2} \to \infty: \quad \theta = Y - 1 = 0\,. \tag{4}$$

On the y-axis we require the standard symmetry conditions

$$x = 0: \quad \partial\theta/\partial x = \partial Y/\partial x = 0\,. \tag{5}$$

Thus, the numerical domain can be reduced to the quarter plane, $x > 0$ and $y > 0$.

When a linear instantaneous concentrated source of thermal energy with intensity $\tilde{E}$ (per unit length) is applied at $x = 0$ and $y = 0$ in an infinite medium, the initial condition at $t = 0$ should be written as $\theta = E\delta(x)\delta(y)$, where $\delta(\cdot)$ is the Dirac δ-function. Here $E = \tilde{E}/[\rho c_p(T_a - T_0)\delta_T^2]$ is a dimensionless amount of energy per unit length of the source.

Without combustion (if $\omega \equiv 0$ is imposed), the temperature field has the well-known analytic solution [18]

$$t > 0: \quad \theta = \frac{E}{4\pi t} \exp\left\{ -\frac{x^2+y^2}{4t} \right\}. \tag{6}$$

In the presence of combustion, the temperature distribution given by Eq. (6) remains valid for $t \ll 1$, since the amount of heat generated by combustion is negligible compared to the initial energy density. The problem of ignition by a single isolated source has been extensively studied in the past. However, for the purposes of completeness of the presentation and comparison of results, this problem considered within the framework of the present model is given in the Appendix.

When the instantaneous linear heat source is placed near a cold wall with a constant temperature at (dimensionless) distance $h = H/\delta_T$ from the wall, then the resulting temperature field is equivalent to the simultaneous application of a virtual source of intensity $-E$ on the other side of the wall, at $y = -h$. In the absence of combustion, the temperature distribution is given by

$$t > 0: \quad \theta = \frac{E}{4\pi t} \exp\left\{ -\frac{(x^2+(y-h)^2}{4t} \right\} - \frac{E}{4\pi t} \exp\left\{ -\frac{(x^2+(y+h)^2}{4t} \right\}. \tag{7}$$

In this work, we will use the value of the thermal dipole intensity defined as $I = 2hE$. When h tends to zero, the value of I will remain finite in order to have a nontrivial result. In other words, as the distance from the source to the wall decreases, the value of E should increase in inverse proportion. Anticipating numerical results, the value of I is decisive for the success or failure of ignition near a cold wall.

The limiting case $h \to 0$ corresponding to a linear concentrated heat source located near an isothermal wall at a distance $H \ll \delta_T$ will be considered first. The temperature distribution at initial moments obtained from Eq. (7) taking the limit $h \to 0$ represents a thermal dipole

$$t \ll 1: \quad \theta = \frac{I\,y}{8\pi t^2} \exp\left\{ -\frac{x^2+y^2}{4t} \right\}, \quad Y = 1, \tag{8}$$

where the dipole intensity is assumed to be a finite value, $I = \lim_{h\to 0} 2hE = const$. It is this temperature distribution that will be used as the initial temperature profile imposed at $t \ll 1$ in this work in order to describe igniting by a thermal dipole.

The following non-dimensional parameters appear in the above formulation: the Zel'dovich number, $\beta = \mathcal{E}(T_a - T_0)/\mathcal{R}T_0^2$, the Lewis number, $Le = \mathcal{D}_T/\mathcal{D}$, the heat release parameter, $\gamma = (T_a - T_0)/T_a$ and the non-dimensional strength of the thermal dipole, $I = 2H\tilde{E}\,/[\rho c_p(T_a - T_0)\delta_T^3]$, evaluated at $H/\delta_T \ll 1$.

The factor $u_p = S_L/U_L$ appearing in Eq. (3) has been introduced to account for the difference between the asymptotic value of the laminar flame speed, $U_L = \sqrt{2\rho\mathcal{B}\mathcal{D}_T Le \beta^{-2}}\exp(-\mathcal{E}/2\mathcal{R}T_a)$, obtained for large activation energy ($\beta \gg 1$) and the numerical value S_L calculated for a finite β. The factor u_p ensures that for a given β the non-dimensional speed of a planar adiabatic flame equals one. Adequate calculation of u_p requires the solution of the following eigenvalue problem

$$\begin{gathered} d\theta/d\xi = d^2\theta/d\xi^2 + \omega, \quad dY/d\xi = Le^{-1}d^2Y/d\xi^2 - \omega, \\ \xi \to -\infty: \quad \theta = Y - 1 = 0, \quad \xi \to +\infty: \quad \theta - 1 = Y = 0, \end{gathered} \tag{9}$$

where ω is given by Eq. (3). In all calculations presented below, the values $\beta = 10$ and $\gamma = 0.7$ are chosen as the most representative. The dependence of u_p on the Lewis number for these values can be found at [19].

3 Numerical treatment

One can see from Eq. (8) that immediately after the energy deposition, at $t \ll 1$, the heated region is small, of order $O(t^{1/2})$. As a consequence, contribution of the combustion heat release remains negligible compared with the energy deposed. In order to provide accurate calculations throughout the initial period, the following transformation was used

$$x = \eta\, e^{\tau/2}\cos\varphi, \quad y = \eta\, e^{\tau/2}\sin\varphi, \quad t = e^{\tau}, \tag{10}$$

where $\eta = \sqrt{x^2+y^2}/\sqrt{t}$ and $0 \le \varphi \le \pi/2$. Using these new variables, Eqs. (1)-(2) take the form

$$\frac{\partial\theta}{\partial\tau} - \frac{\eta}{2}\frac{\partial\theta}{\partial\eta} = \frac{1}{\eta}\frac{\partial}{\partial\eta}\left(\eta\frac{\partial\theta}{\partial\eta}\right) + \frac{1}{\eta^2}\frac{\partial^2\theta}{\partial\varphi^2} + e^{\tau}\omega, \tag{11}$$

$$\frac{\partial Y}{\partial\tau} - \frac{\eta}{2}\frac{\partial Y}{\partial\eta} = \frac{1}{Le}\left\{\frac{1}{\eta}\frac{\partial}{\partial\eta}\left(\eta\frac{\partial Y}{\partial\eta}\right) + \frac{1}{\eta^2}\frac{\partial^2 Y}{\partial\varphi^2}\right\} - e^{\tau}\omega. \tag{12}$$

The initial conditions applied for $t \ll 1$ correspond to $\tau \to -\infty$. Thus, appropriate initial conditions for Eqs. (11)-(12) obtained from Eq. (8) become

$$\tau \to -\infty: \quad \theta = \frac{I\eta\sin\varphi}{8\pi}\exp\left\{-\frac{\eta^2}{4} - \frac{3}{2}\tau\right\}, \quad Y = 1. \tag{13}$$

One can see that the reaction rate term given by Eq. (3) is bounded as $\theta \to \infty$, namely $\omega(\theta, Y) < \beta^2 e^{\beta/\gamma}/2Le u_p^2$, and the term $e^{\tau}\omega$ appearing in Eqs (11)-(12) becomes negligible as $\tau \to -\infty$ (or $t \ll 1$). In the absence of combustion, namely if we put $\omega = 0$ in Eq. (1), the dependence of the maximum temperature on time obtained from the distribution given by Eq. (8) is expressed as

$$\theta_{max} = \frac{e^{-1/2}\sqrt{2}\, I}{8\pi t^{3/2}}\,. \tag{14}$$

This dependence can be used as an additional accuracy checking of calculations.

The above transformation makes it possible to adjust the numerical domain at the initial stage of the process to the hot region size which increases in time as $\sqrt{t}$ (where, in fact, ignition takes place), as well as to have a sufficiently small time step during this initial stage for the physical time variable t. Indeed, given a uniform step $\delta\tau$ for variable τ, the step for the physical time variable, $\delta t = e^{\tau}\delta\tau$, becomes automatically small when $\tau \to -\infty$.

Computations were carried out in a finite domain, $0 \leq \eta \leq \eta_{max}$, and the initial conditions (13) were imposed for $\tau = \tau_{min}$. Values $\eta_{max} = 15 \div 40$ and $\tau_{min} = -(5 \div 10)$ were used as typical ones. All the numerical results reported below were obtained using second-order, three-points central differences for spatial derivatives on a rectangular uniform grid with a typical resolution of $\delta\eta = \eta_{max}/(500 \div 1000)$ and $\delta\varphi = 2\pi/(100 \div 200)$. An explicit in η and implicit in φ marching procedure was used with first order discretization in time where the Thomas algorithm was used. The presence of the highly nonlinear reaction rate terms required to choose a sufficiently small time step, $\delta\tau = 10^{-4} \div 10^{-5}$. The independence of the results on $\delta\eta$, $\delta\varphi$ and $\delta\tau$ was verified specifically.

To track the advancement of the combustion wave, we will use the position of the front, y_f, along the y-axis, that is, the axis perpendicular to the wall. This value is determined by the point at which the burning rate reaches its maximum value, $\omega_{max} = \omega_{(x=0,y=y_f)}$.

It is also convenient to use the values of the maximum temperature along the y-axis, θ_{max}, to identify successful or unsuccessful ignition. Anticipating numerical results, the maximum value of the temperature along the y axis always coincides with the maximum value in the domain for $Le \geq 1$. However, this is not always the case for $Le < 1$. Nevertheless, the maximum temperature value along the y-axis is quite representative.

The ignition process is considered successful when θ_{max} remains close to unity as $t \gg 1$.This corresponds to the appearance of a combustion front propagating from the point of the source application. The front propagation velocity becomes of the order of unity in dimensionless variables, i.e. $y_f \sim t$. This means that the use of transformed coordinates given by Eq. (10) becomes less efficient at $t \gg 1$, as the position of the front in new coordinates is $\eta_f = y_f/\sqrt{t} \sim \sqrt{t}$ thus approaching η_{max}. This requires the selection of large values for η_{max}, thereby reducing the accuracy of the calculations. Calculations were interrupted when $\eta_f = 0.7\,\eta_{max}$. The ignition

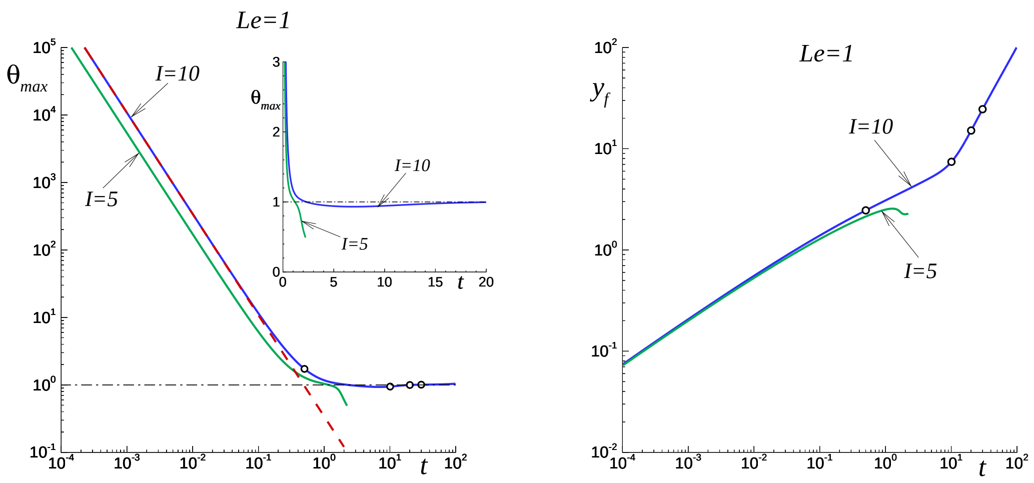

Figure 1: Time histories of the maximum temperature in the computational domain (left plot) and the flame position along the y-axis (right plot) for $I = 10$ (successful ignition) and $I = 5$ (ignition failed). The dashed line in the left figure shows the maximum temperature given by Eq. 14 plotted for $I = 10$. Open circles indicate the points corresponding to the distributions in Figure 2.

process was considered unsuccessful if the maximum temperature fell below $\theta_{max} < 0.5$. After this moment, the calculations were also stopped.

4 Results

4.1 The case $Le = 1$

Figure 1 shows two cases illustrating successful (the curve with $I = 10$) and unsuccessful (the curve with $I = 5$) ignition processes calculated for $Le = 1$. The left plot shows the maximum temperature versus time. For the main figure, logarithmic axes are used, and the inset shows the dependencies on t. The dashed line represents the dependence of the maximum temperature on time given by Eq. (14) plotted for $I = 10$. It can be seen that at $t \ll 1$ the solid and dashed lines coincide with a very high accuracy. The right plot shows the time dependence of the flame position along the y-axis for the same values of the dipole intensity.

Figure 2 illustrates the temperature (solid lines) and mass fraction (dashed lines) distributions along the y-axis at different times. These moments correspond to the open circles shown in

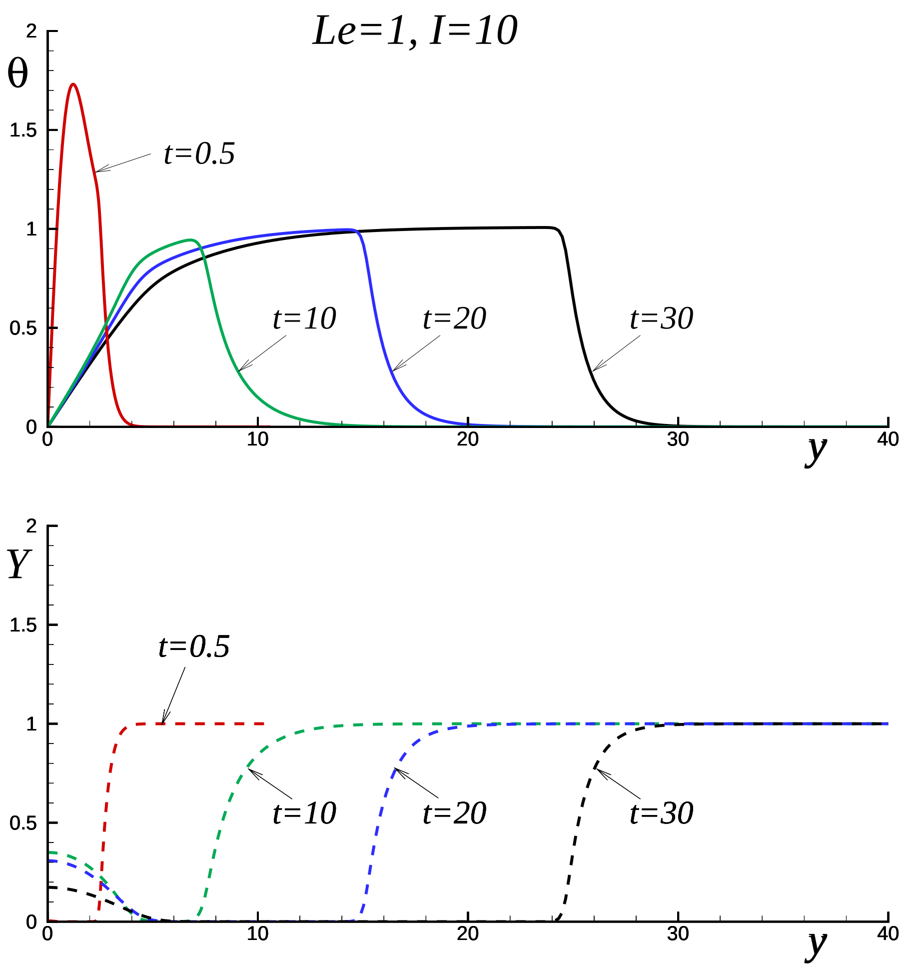

Figure 2: Distributions of temperature (upper plot) and mass fraction (lower plot) for ignition by a dipole, for $Le = 1$ and $I = 10$ at the times indicated by open circles in Figure 1.

Figure 1. It can be seen that over a fairly long time, a combustion front with a temperature close to unity is forming and propagates with a velocity close to unity. The leading part of the temperature front is practically separated from the rear of the temperature distribution, where the width of the heat loss zone increases approximately as $\sqrt{t}$.

It is interesting also to note the appearance of a zone with a nonzero mass fraction near the wall at sufficiently long times. This is due to the cooling of the mixture near the wall with the subsequent diffusion of the fuel along the x-axis. It can be also noted that the maximum temperature takes its minimum value at about $t \approx 10$ and then approaches unity. This temporary temperature minimum can also be seen in Fig. 1 (left).

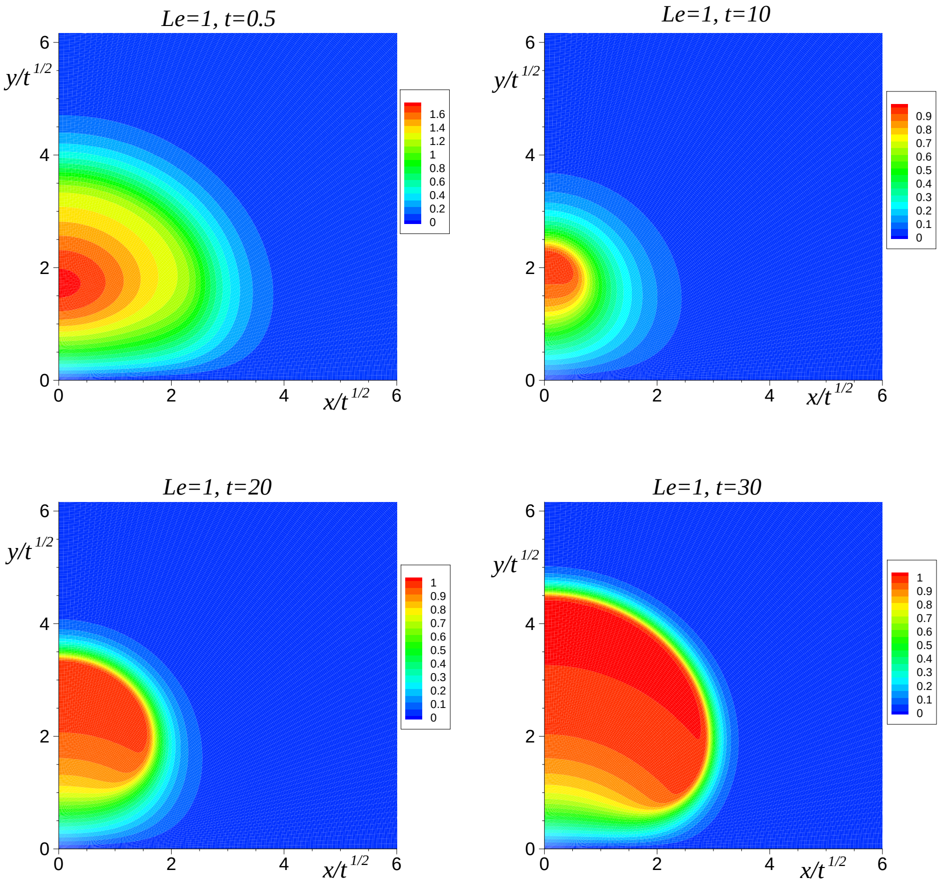

Figure 3: Temperature distributions obtained during ignition by a thermal dipole plotted in variables $x/\sqrt{t}$ and $y/\sqrt{t}$ for different times; all plots for $I = 10$, $Le = 1$.

Figure 3 illustrates the spatial temperature distributions for the times indicated by the open circles in Fig. 1. One can appreciate the advantage of using the transformed coordinates $(x/\sqrt{t}$, $y/\sqrt{t})$ over purely Cartesian coordinates (x, y): the reaction zone evolves slowly in terms of the new variables at the initial stage of the process when the success or failure of ignition is determined.

4.2 Influence of the Lewis number

All the results presented above describe the flame dynamics for $Le = 1$. It is well known that when the Lewis number deviates from unity, it has a strong effect on the propagating flame structure. For example, for curved flames with $Le < 1$ zones with temperatures higher than the

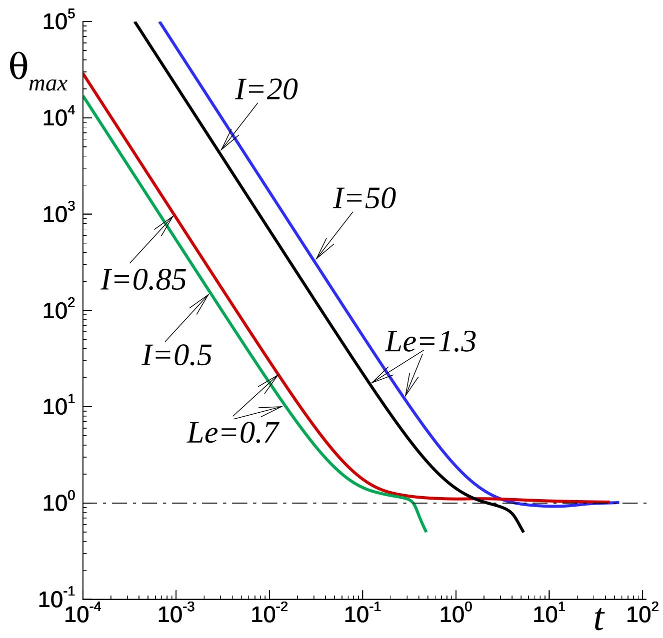

Figure 4: Time histories of the maximum temperature calculated for $Le = 1.3$ and 0.7 for different values of the dipole intensity.

adiabatic temperature appear.

From a qualitative point of view, the dynamics of the flame initiation for Lewis numbers other than unity occurs in the same manner as described above. Figure 4 shows the maximum temperature versus time calculated for $Le = 1.3$ and 0.7. For both cases, the curves calculated for two dipole intensities are drawn, one for successful ignition and the other for failed ignition.

Still, it should be noted that at large time the flame structure after ignition at a Lewis number less than one becomes different from that at $Le = 1$. Figure 5 shows examples of the temperature distributions after successful ignition calculated for $Le = 0.3$, $I = 10^{-3}$ and plotted for $t = 0.5$ (left plot) and $t = 16.6$ (right plot). The color shows the temperature field, and the solid white lines specifically denote the temperature contours with $\theta = 1$, 1.25 and 1.35 in the left plot and $\theta = 1$, 1.05, 1.1 and 1.15 in the right plot. It can be seen that, in comparison with the temperature distributions obtained for $Le = 1$, where the maximum temperature is achieved on the y-axis, the maximum temperature for $Le = 0.3$ can be found near the wall where the flame curvature is maximum. However, it should be noted that this is less noticeable in the early

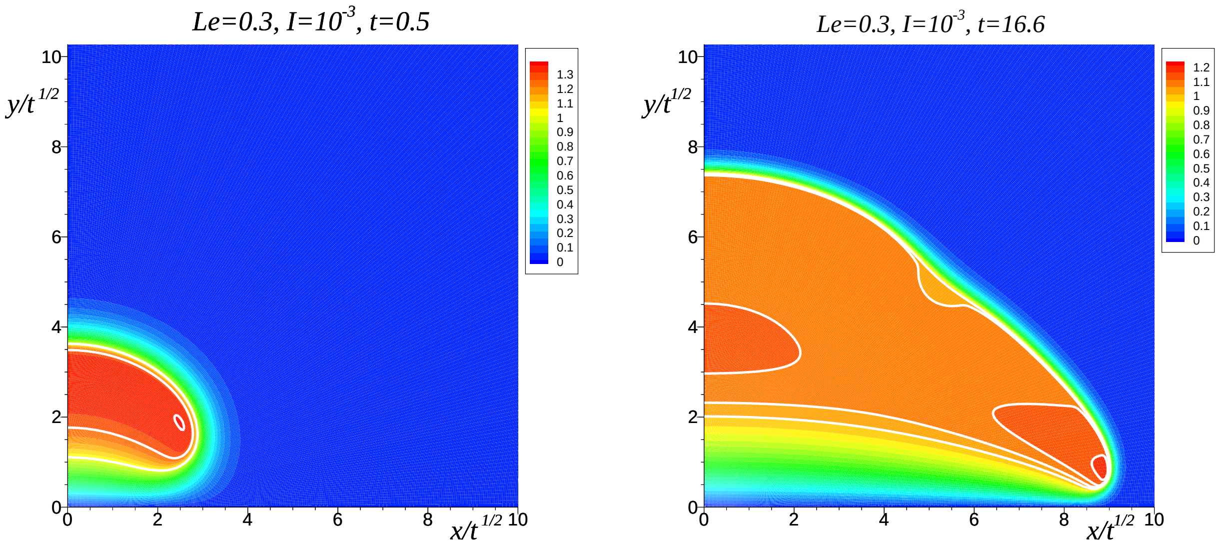

Figure 5: Temperature distribution after successful ignition at $Le = 0.3$, $I = 10^{-3}$, for $t = 0.5$ and $t = 16.6$. White contour lines indicate isotherms with $\theta = 1$, 1.25 and 1.35 in the left plot and $\theta = 1$, 1.05, 1.1 and 1.15 in the right plot.

stages of flame ignition, when the effect of heat release due to combustion has not yet become a determining factor.

It is also interesting to note that flame propagation along the cold wall occurs at a higher speed than in the direction perpendicular to the wall, where there are no heat losses. This is also associated with the appearance of the hottest gas temperature near the wall due to the effect of Lewis number less than one and flame curvature.

The main effect produced by the variations of the Lewis number is a significant change in the critical value of the dipole intensity above which ignition is successful, I_c. Figure 6 shows this relationship using a logarithmic scale for I_c. It can be seen that the critical value can change by several orders of magnitude when the Lewis number changes.

4.3 The cases of finite h

It is interesting to compare the ignition process due to the thermal dipole with the ignition from a linear instantaneous source placed at a finite distance from the isothermal wall, $h = O(1)$. For this, the initial distributions given by Eq. 7 were used. To make the comparison easier, the

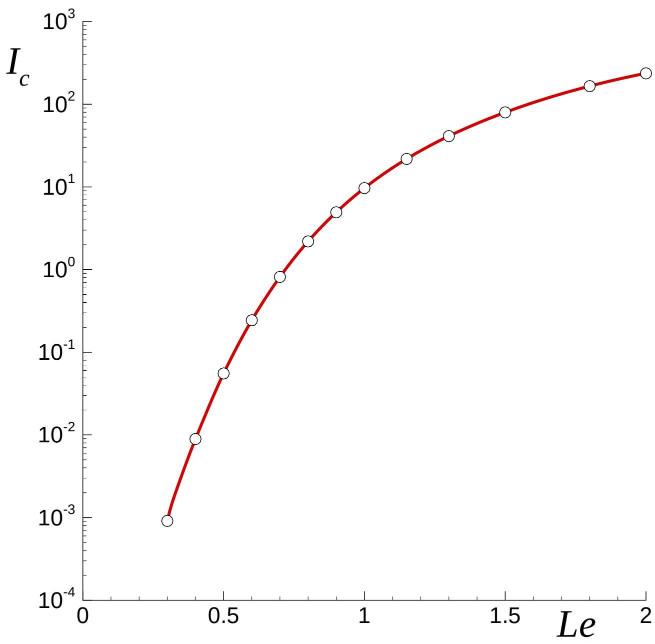

Figure 6: The critical value of the dipole intensity, I_c, above which the ignition process is successful plotted as a function of the Lewis number, for $\beta = 10$ and $\gamma = 0.7$.

thermal energy was set as $E = I/2h$, where I was fixed. This makes it possible to compare the cases with different values of h, including the limiting case $h \ll 1$. The corresponding minimum energy for successful ignition can be calculated as $E_c = I_c/2h$.

Figure 7 shows the temperature and mass fraction distributions along the y-axis for ignition obtained from a linear instantaneous source located at $h = 1$. The source intensity, equal to $E = 5$ which corresponds to $I = 10$, is the same as in Fig. 2. One can see that, except for very short times, the variable distributions become very similar. Figure 8 illustrates spatial temperature distributions for several instants. At the initial moments of time, the visible shift of the position of the hot spot occurs due to the transformation of coordinates: in ordinary coordinates, (x, y), the size of the domain grows as $\sqrt{t}$.

The dependence of the maximum temperature on time is shown in Fig. 9 by solid lines for successful ($I = 10$) and unsuccessful ($I = 6.5$) ignition, both for $h = 1$. The dashed line shows the θ_{max}-dependence in the absence of combustion for $I = 10$ given by $\theta_{max} = I/(8\pi h t)$. Excellent agreement between the solid and dashed curves at short times can be observed.

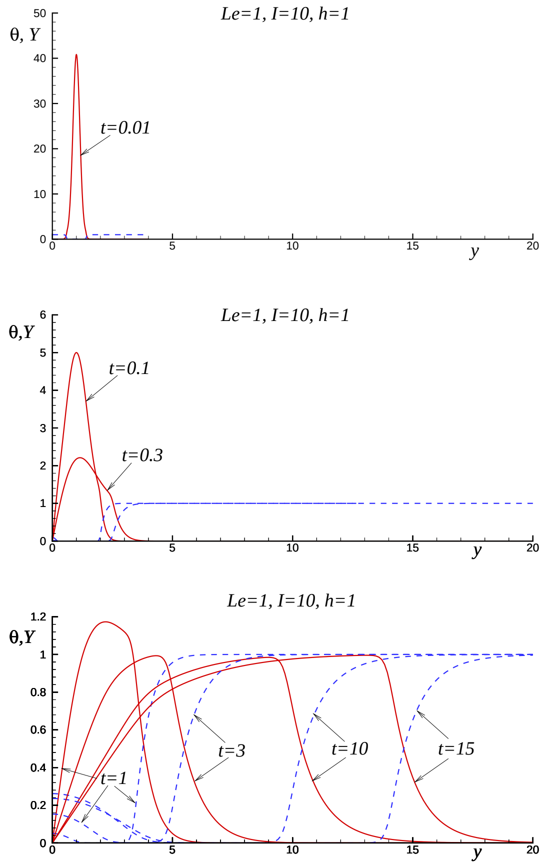

Figure 7: Distributions along the y-axis of temperature (solid lines) and mass fraction (dashed lines) for ignition from an instantaneous source located at a finite distance, h, from a cold wall; calculated for $I = 10$, $h = 1$.

Figure 10 shows with solid lines the critical value I_c (left plot) and the critical thermal energy, $E_c = I_c/(2\,h)$ (right plot), above which ignition is successful, as functions of h, all curves calculated for $Le = 1$. Open delta-symbols indicate the calculated values. An open circle indicates the value of I_c obtained when $h \to 0$. The dashed-dotted straight lines in both plots show the asymptotic dependencies, namely $I_c = 2hE_c$ in the left plot, obtained from the ignition calculations by the isolated source given in the Appendix. For the dipole intensity dependence, it is $I_c = 1.145 \cdot h$, and for the critical energy, it is $E_c \approx 0.5725$. The dashed line in the right figure shows the asymptotic dependence of the critical energy on h for $h \ll 1$ obtained from the thermal dipole calculations, $E_c = 4.835/h$.

Critical I_c values calculated for Lewis numbers smaller and larger than one are shown in

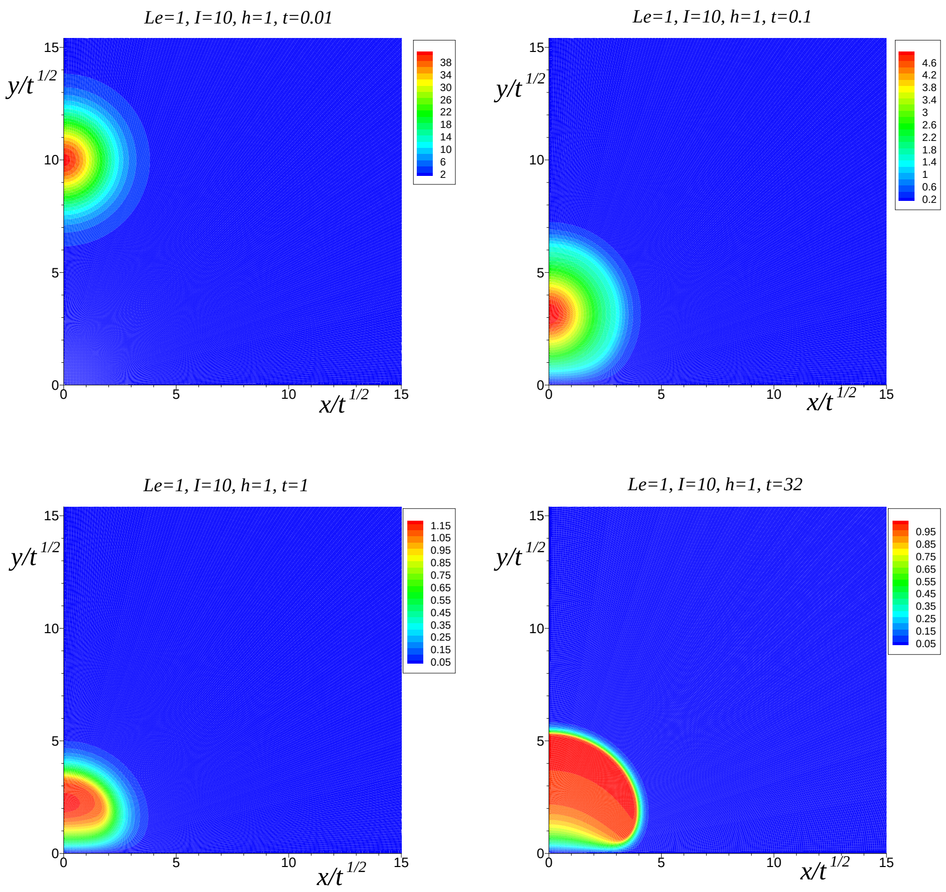

Figure 8: The spatial temperature distributions plotted in variables $x/\sqrt{t}$ and $y/\sqrt{t}$ drawn for different moments of time during ignition from an instantaneous source located at a distance $h = 1$ from the wall, for $I = 10$ ($E = 5$).

Fig. 11 by solid lines as function of h. The dashed lines show the asymptotic dependence $I_c = 2hE_c$, where E_c is obtained from the results of ignition by an isolated heat source. Open circles in both plots indicate the values of I_c obtained when $h \to 0$.

The minimum of the solid curves in these figures, as well as in Fig. 10 (left), indicate unmistakably the critical value of the distance from the source to the wall, h_c, beyond which the presence of a cold wall no longer affects ignition. Indeed, the dependence of I_c on h approaches the asymptotic $I_c = 2hE_c$ immediately after this minimum (for Le larger than one, this happens a little further), where E_c is determined by the critical value for successful ignition by an isolated source, see Appendix. The values of h_c are shown in Fig. 12 as a function of the Lewis number.

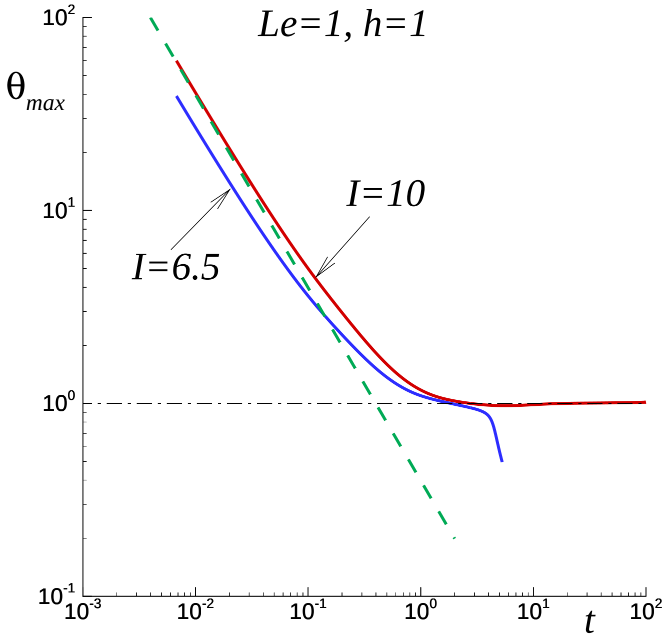

Figure 9: Maximum temperature as a function of time (solid lines) for successful ($I = 10$) and unsuccessful ($I = 6.5$) ignitions, calculated for $Le = 1$ and $h = 1$; a dashed line shows the maximum temperature in the absence of combustion ($\omega \equiv 0$) for $I = 10$.

An important dependence of h_c on the Lewis number should be noted.

5 Discussions and conclusions

Under realistic conditions, ignition of a combustible mixture is rarely possible without the accompanying loss of applied thermal energy. The presence of walls or other solid conducting bodies of high heat capacity near the place of flame initiation is often inevitable. As a consequence, a significant portion of the energy required for ignition is often lost. This fact is usually ignored in studies to determine the minimum heat energy required for a successful ignition process. In this paper, we are trying to fill this gap.

The case of instantaneous application of thermal energy (for example, a spark) near the wall is considered as a model situation. In the model under consideration, a number of simplifications are allowed, which, however, are not too exotic, being widely used in studies of the ignition

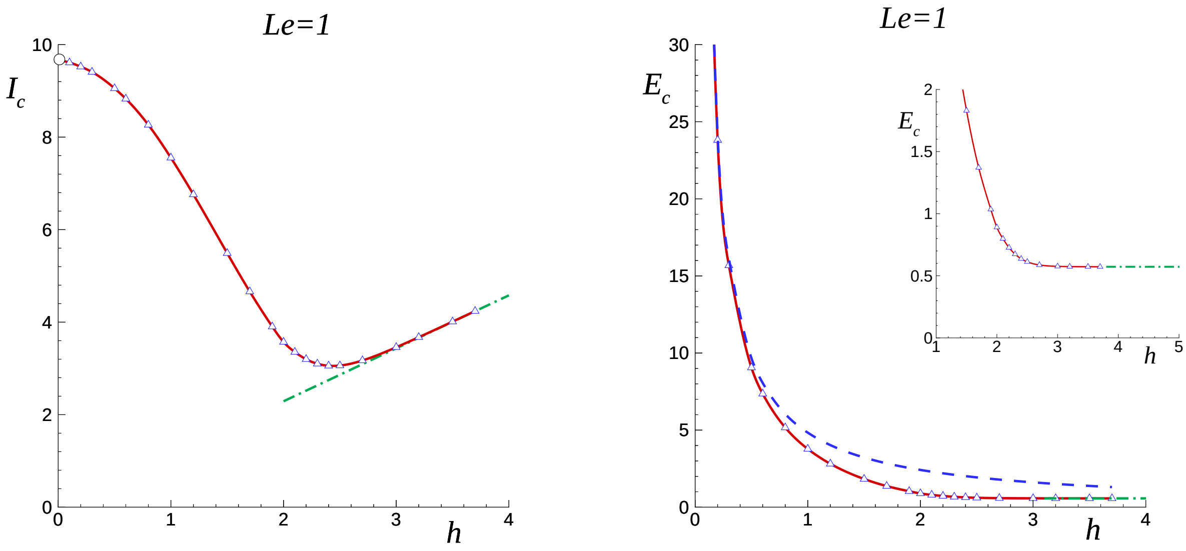

Figure 10: Solid lines with triangles show the critical dipole intensity, I_c (left plot), and the minimum ignition energy, $E_c = I_c/(2\,h)$ (right plot), as a function of h, for $Le = 1$; a dashed line in the right plot shows the asymptotic curve $E_c = 4.835/h$ calculated for $h \ll 1$ based on the thermal dipole approximation; dash-dot lines in the left and right plots show $I_c = 1.145 \cdot h$ and $E_c = 0.5725$, respectively, obtained for $h \gg 1$ (see the Appendix).

phenomenon. Another motivation for using simplified models is to reduce the number of control parameters affecting the process. Specifying these parameters would require a narrower and more specific choice for them. The weakening of the simplifying assumptions enumerated below will be carried out in further research.

First of all, it should be noted that the wall temperature was maintained constant, always remaining cold. This assumption can be easily accepted if the heat capacity properties of the wall material are high, especially in the early stages of the process. On the other hand, weakening this assumption does not present serious difficulties.

Another significant assumption is the use of a diffusive-thermal model in which density changes are ignored. It should be noted that models with constant density are widely used in the study of ignition processes, since flame initiation is more related to the interaction between heat transfer and chemical transformation processes. This simplification also effectively eliminates the consideration of hydrodynamic effects.

One of the significant differences in this formulation of flame initiation near the wall is the

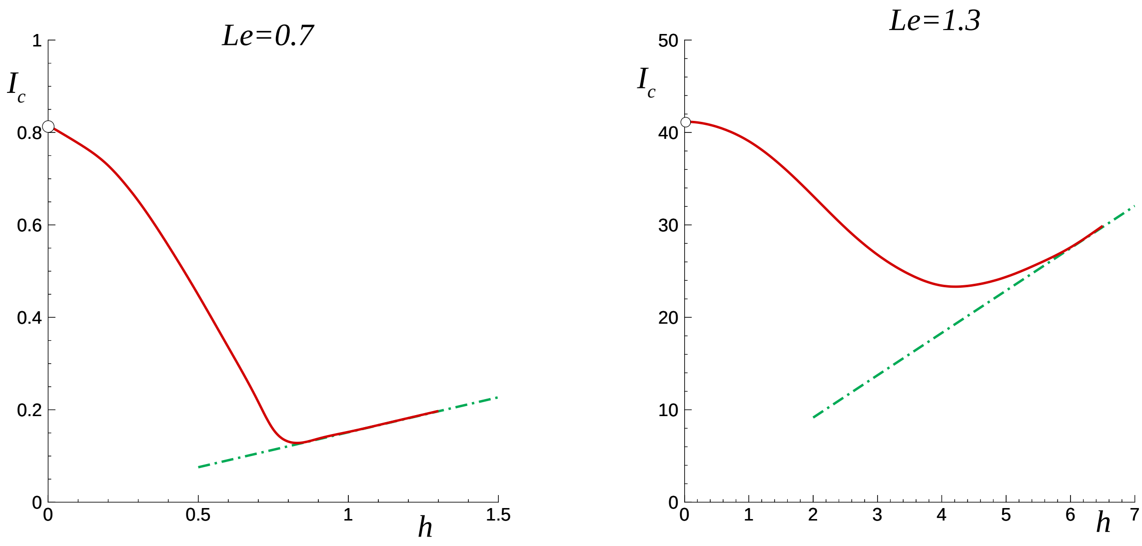

Figure 11: Critical values of the dipole intensity, I_c, for $Le = 0.7$ (left plot) and $Le = 1.3$ (right plot) as functions of h; dash-dotted lines in both plots show the asymptotic dependence $I_c = 2hE_c$ with E_c given in Fig. 14 (see the Appendix).

spatial multidimensionality of the problem. The vast majority of work on ignition has been done under the assumption of perfect symmetry, in other words, only one spatial variable was considered. Finally, the authors believe that the use of stretched coordinates in the present work made it possible to significantly improve and refine the consideration of the ignition process from a concentrated source of thermal energy. In fact, at short times when the success of the ignition process is decided, this transformation allows the process to follow more naturally, thus reducing the size of the required numerical domain.

In the extreme case of short proximity of the source to the wall, the source acts in the manner of a thermal dipole. It has been demonstrated in this work that with a sufficient intensity of the latter, a successful ignition process can indeed be carried out. An interesting result is the strong dependence, up to several orders of magnitude, of the critical intensity of the dipole for successful ignition on the Lewis number. The physical interpretation of this result undoubtedly resembles the appearance of super adiabatic temperatures in the case of a ball flame at low Lewis numbers.

A noticeable feature that appears after ignition near a cold wall at Lewis numbers less than one is a higher flame propagation speed along the wall direction than in the direction perpen-

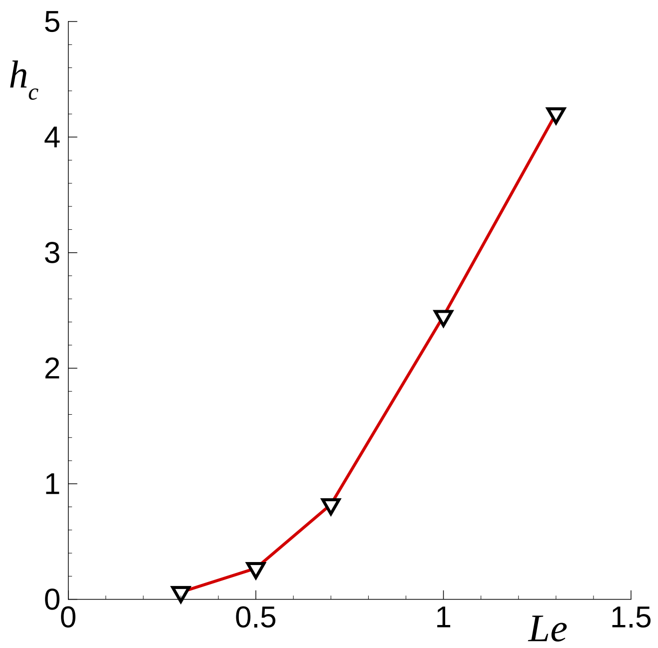

Figure 12: Approximate values of the distance from wall to source (values at which the curves shown in Fig. 10 (left) and Fig. 11 have a minimum), h_c, as a function of the Lewis number. For $h > h_c$ the cold wall ceases to affect the ignition.

dicular to it. This unexpected result is associated with the effect of flame curvature appearing at $Le < 1$ due to heat losses occurring near the cold wall. Obviously, this will not be the case for ignition near an adiabatic wall.

As is often the case when using asymptotic procedures, the applicability of these procedures is not limited only to strict adherence to the smallness of the expansion parameter. In the case of ignition near a cold wall, the results of ignition with a dipole can also be used in situations where the distance between the source and the wall is not infinitesimal. It is shown that the minimum thermal energy for ignition increases in inverse proportion to the wall distance, which is an acceptable criterion for a priori assessment of ignition success. Another important result was that the minimum energy for successful ignition becomes independent of the distance to the cold wall at $h > h_c$. In these cases, it becomes equal to the minimum ignition energy in the case of an isolated heat source.

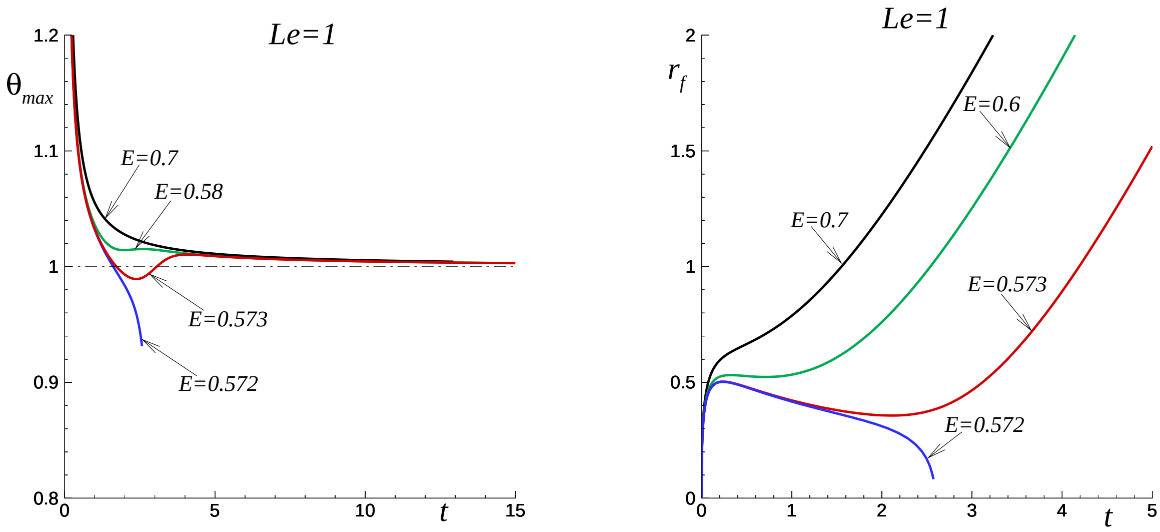

Figure 13: Examples of the maximum temperature (left plot) and flame position (right plot) on time for successful and successful ignition using an isolated source in an infinite medium; all curves for $Le = 1$.

Acknowledgement

This work was financed by project #PID2019-108592RB-C41-C42 / AEI / 10.13039/501100011033.

Appendix. Single source ignition

The problem of ignition by an isolated source of thermal energy placed in an infinite medium has been considered many times from different points of view. In this Appendix, we present the results obtained within the framework of the model used in this study. This is for ease of comparison of the results.

A counterpart of Eqs. (11)-(12) written for the axisymmetric case ($\partial/\partial\varphi \equiv 0$ is imposed) was solved numerically. The initial conditions (6) were used as follows

$$\tau \to -\infty: \quad \theta = \frac{E}{4\pi} \exp\left\{ -\frac{\eta^2}{4} - \tau \right\}, \quad Y = 1\,.$$

Figure 13 shows the time histories of the maximum temperature (left plot) and flame position (right plot) for $Le = 1$ and various values of E. The variation of the critical ignition energy, E_c,

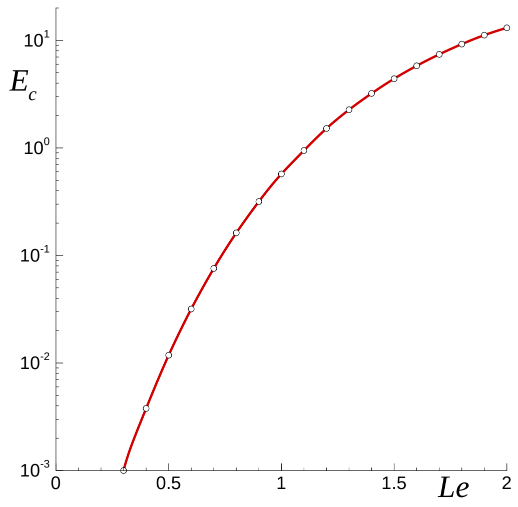

Figure 14: The critical energy, E_c, above which the ignition process is successful for an isolated source in an infinite medium, as a function of the Lewis number, calculated for $\beta = 10$ and $\gamma = 0.7$.

above which ignition is successful is shown as a function of the Lewis number in Fig. 14. In particular, the critical value of the energy for ignition is $E_c = 0.5725$ for $Le = 1$.

References

[1] R.S. Silver, The ignition of gaseous mixtures by hot particles, *Phil. Mag. J. Sci.* 23(156) (1937) 633-657.

[2] H.P. Stout, Mechanism of ignition by local sources of heat, *Nature* 166 (1950) 28-29.

[3] B. Lewis, G. von Elbe, Combustion, Flames and Explosions of Gases, 2. Auflage. Academic Press Inc. New York und London 1961.

[4] G. Dixon-Lewis, I.G.Shepherd, Some aspects of ignition by localized sources, and of cylindrical and spherical flames, *Proc. Combust. Inst.* 15 (1975) 1483-1491.

[5] G. Dixon-Lewis, Effect of core size on I ignition energy by localized sources, *Combust. Flame* 33 (1978) 319-321.

[6] K. Kalkasanath, E. Oran, J. Boris, A theoretical study of the ignition of premixed gase, *Combust. Flame* 47 (1982) 173-190.

[7] P.S.Tromans, R.M.Furzeland, An analysis of Lewis number and flow effects on the ignition of premixed gases, *Proc. Combust. Inst.* 21 (1988) 1891-1897.

[8] A. Frendi, M. Sibulkin, Dependence of minimum ignition energy on ignition parameters, *Combust. Sci. Tech.* 73 (1990) 395-413.

[9] B. Deshaies, G. Joulin, On the initiation of a spherical flame kernel, *Comust. Sci. Tech.* 37 (1984) 99-116.

[10] G. Joulin, Point-source initiation of lean spherical flames of light reactants: an asymptotic theory, *Combust. Sci. Tech* 43 (1985) 99-113.

[11] L. He, Critical conditions for spherical flame initiation in mixtures with high Lewis numbers, *Combust. Theor. Modell.* 4 (2000) 159-172.

[12] C. Vázquez-Espí, A. Liñán, Thermaldiffusive ignition and flame initiation by a local energy source, *Combust. Theor. Modell.* 6 (2002) 297-315.

[13] V. Kurdyumov, J. Blasco, A.L. Sánchez, A. Liñán, On the calculation of the minimum ignition energy, *Combust. Flame* 136 (2004) 394-397.

[14] Z. Chen, Y. Ju, Theoretical analysis of the evolution from ignition kernel to flame ball and planar flame, *Combust. Theor. Modell.*, 11 (2007) 427-453.

[15] Z. Chen, M.P. Burke, Y. Ju, On the critical flame radius and minimum ignition energy for spherical flame initiation, *Proc. Comust. Inst.* 33 (2011) 1219-1226.

[16] E. Fernández-Tarrazo, M. Sánchez-Sanz, A.L. Sánchez, F.A. Williams, Minimum ignition energy of methanol-air mixtures, *Combust. Flame* 171 (2016) 234-236.

[17] M. Sánchez-Sanz, E. Fernández-Tarrazo, A.L. Sánchez, Regimes of boundary-layer ignition by heat release from a localized energy source, *Proc. Combust. Int.* 34 (2017) 1467-1473.

[18] A.N. Tikhonov, A.A. Samarskii, Equations of Mathematical Physics, Pergamon Press: Oxford, 1963.

[19] V.N. Kurdyumov, Lewis number effect on the propagation of premixed flames in narrow adiabatic channels: Symmetric and non-symmetric flames and their linear stability analysis, *Combust. Flame* 158 (2011) 1307-1317.